



**HAL**  
open science

## **Straightforward N -Acyl Homoserine Lactone Discovery and Annotation by LC–MS/MS-based Molecular Networking**

Alice M S Rodrigues, Raphaël Lami, Karine Escoubeyrou, Laurent Intertaglia, Clément Mazurek, Margot Doberva, Pedro Pérez-Ferrer, Didier Stien

► **To cite this version:**

Alice M S Rodrigues, Raphaël Lami, Karine Escoubeyrou, Laurent Intertaglia, Clément Mazurek, et al.. Straightforward N -Acyl Homoserine Lactone Discovery and Annotation by LC–MS/MS-based Molecular Networking. *Journal of Proteome Research*, 2022, 21, pp.635-642. 10.1021/acs.jproteome.1c00849 . hal-03551975

**HAL Id: hal-03551975**

**<https://hal.science/hal-03551975>**

Submitted on 2 Feb 2022

**HAL** is a multi-disciplinary open access archive for the deposit and dissemination of scientific research documents, whether they are published or not. The documents may come from teaching and research institutions in France or abroad, or from public or private research centers.

L'archive ouverte pluridisciplinaire **HAL**, est destinée au dépôt et à la diffusion de documents scientifiques de niveau recherche, publiés ou non, émanant des établissements d'enseignement et de recherche français ou étrangers, des laboratoires publics ou privés.

# **Straightforward *N*-Acyl Homoserine Lactone Discovery and Annotation by LC-MS/MS-based Molecular Networking**

Alice M. S. Rodrigues,<sup>\*,1,2</sup> Raphaël Lami,<sup>1</sup> Karine Escoubeyrou,<sup>1,2</sup> Laurent Intertaglia,<sup>1,2</sup> Clément Mazurek,<sup>1</sup> Margot Doberva,<sup>1</sup> Pedro Pérez-Ferrer,<sup>1</sup> Didier Stien<sup>1</sup>

<sup>1</sup>Sorbonne Université, CNRS, Laboratoire de Biodiversité et Biotechnologies Microbiennes, LBBM, Observatoire Océanologique, 66650, Banyuls-sur-mer, France.

<sup>2</sup>Sorbonne Université, CNRS, Fédération de Recherche, Observatoire Océanologique, 66650, Banyuls-sur-mer, France.

\*Email: [rodrigues@obs-banyuls.fr](mailto:rodrigues@obs-banyuls.fr)

**ABSTRACT:** *N*-Acyl-L-homoserine lactones (AHLs) are a large family of signaling molecules in ‘quorum sensing’ communication. This mechanism is present in a number of bacterial physiological phenomena, including pathogenic phenomena. In this study, we described a simple and accessible way to detect, annotate and quantify these compounds from bacterial culture media. Analytical standards and ethyl acetate bacterial extracts containing AHLs were analyzed by a UHPLC system coupled to a mass spectrometer using a nontargeted FullMS data-dependent MS<sup>2</sup> method. The results were processed in MZmine2 and then analyzed by a FBMN workflow in the GNPS platform for discovery and annotation of known and unknown AHLs. Our group analyzed 31 AHL standards and included the MS<sup>2</sup> spectra in the spectral library of the GNPS platform. We also provide the 31 standard AHL spectrum list for inclusion in molecular networking analyses. FBMN analysis annotated 30 out of 31 standards correctly. Then, as an example, a set of five bacterial extracts was prepared for AHL annotation. Following the method described in this article, five known and 11 unknown AHLs were properly annotated using the FBMN-based molecular network approach. This study offers the possibility for the automatic annotation of known AHLs and the search for nonreferenced AHLs in bacterial extracts in a somewhat straightforward approach even without acquiring analytical standards. The method also provides relative quantification information.

**Keywords.** *N*-Acyl-L-homoserine lactones (AHLs), quorum sensing, automatic annotation, molecular network (MN).

## INTRODUCTION

*N*-Acyl-L-homoserine lactones (AHLs, Figure 1) are a very diverse group of structurally related compounds known to play important roles as signaling molecules in cell-to-cell communication. This type of communication has been particularly studied in bacteria and is also named ‘quorum sensing’. Indeed, it has been demonstrated that AHLs accumulate in the nearby environment of cells and, when a sufficient concentration is reached, regulate a wide range of physiological activities in the entire population that can ‘sense’ these molecules.<sup>1</sup> This mechanism allows the coordination of a wide range of physiological activities, including biofilm formation, conjugation, and nutrient acquisition.<sup>2</sup> Quorum sensing systems are extremely diverse and not solely restricted to bacteria. However, the emission of AHL signaling is widespread, and AHL synthases were found in very diverse bacteria, including *Vibrio*, *Roseobacter*, *Actinobacteria* and *Pseudomonas*.<sup>3</sup> The capacity to perceive such signals has been reported in bacteria as well as in many eukaryotic species.<sup>4</sup>

All AHLs are comprised of a homoserine lactone moiety derived from amino acid metabolism linked to an acyl side chain originating from fatty acid biosynthesis. The variability and the species selectivity of AHLs is linked to the nature of the fatty acid side chain. The AHLs can differ with regards to three characteristics of the *N*-acyl chains: (i) the length, from 2 to 18 or more carbons; (ii) the possible substitution at the 3-position; and (iii) the presence of carbon-carbon double bonds.<sup>5</sup>

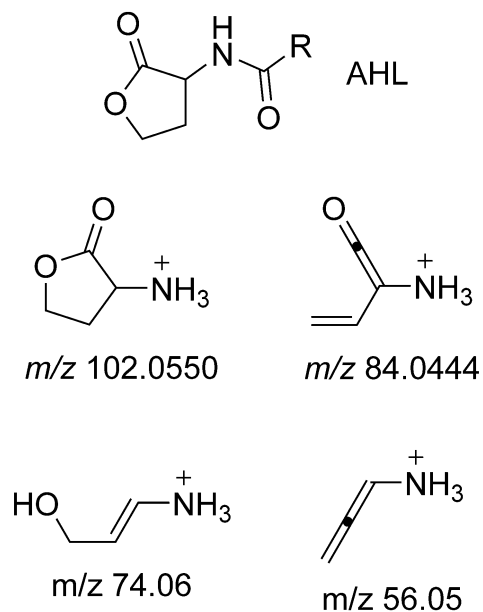


**Figure 1.** AHL general formula in which R is a fatty acid, and AHLs common fragments in MS<sup>2</sup>

Due to the structural heterogeneity of AHLs, several technical approaches have been reported in the literature to determine their identity and concentration from different matrices. Bacterial biosensors,<sup>6</sup> gas chromatography–mass spectrometry (GC–MS/MS), Fourier transform ion cyclotron resonance (FTICR)<sup>7</sup> and mass spectrometry coupled in-line with HPLC<sup>8–10</sup> have been used most often. However, data are usually processed manually, and the detection and annotation of unprecedented AHLs is often not straightforward. In the current study, we provide a rapid, reliable and accessible method for the detection and annotation of known and unknown AHLs in bacterial culture and bacteria-rich media. The detection is based on the construction of a MN from nontargeted fragmentation profiles obtained by UHPLC-high resolution mass spectrometry after we implemented the GNPS database with many AHL MS<sup>2</sup> spectra. The method does not require analytical standards.

## EXPERIMENTAL SECTION

### Chemicals and solvents

*N*-Acyl-homoserine lactone analytical standards were obtained from Cayman Chemical (Ann Arbor, MI, United States). Stock solutions of each AHL were prepared by dissolving commercial standards in methanol (or dichloromethane for C18-AHL) at a concentration of 1 mg/mL and were stored at  $-80^{\circ}\text{C}$ . Solutions of mixed standards for UHPLC-HRMS analyses were prepared by diluting stock solutions with methanol to generate a set of standard solutions with AHL concentrations ranging from 2,000 to 2 ng/mL. The list of standard AHLs is provided in Table 1. Standard solutions were used to determine the limits of detection (LODs) and chromatographic retention times and to draw external calibration curves for AHL quantification. LC-MS grade methanol, acetonitrile and formic acid were purchased from Biosolve (Biosolve Chimie France, Dieuze), and analytical-grade ethyl acetate was obtained from Sigma-Aldrich. Pure water was obtained from an Elga Purelab Flex system (Veolia LabWater STI, Antony, France).

### Bacterial culture and extraction of AHLs

Five different *Rhodobacteraceae* strains from the Banyuls Bacterial Culture Collection<sup>11</sup> were selected for this study: two *Paracoccus* sp., BBCC191 and BBCC192, and three *Phaeobacter* sp., BBCC442, BBCC445 and BBCC1957 (affiliation based on their 16SrRNA gene sequence). *Rhodobacteraceae* are likely to produce AHLs.<sup>2,8</sup> These strains were precultured (96 h,  $25^{\circ}\text{C}$ , 100 rpm) in 30 mL of marine broth (MB, Difco 2216). Then, 5 mL of this preculture was transferred to a fresh 50 mL of MB in an Erlenmeyer flask in triplicate (200 rpm,  $20^{\circ}\text{C}$ ). After 72 h (late exponential growth phase), ethyl acetate (50 mL) was added to the flask. The extraction protocol was adapted from that described previously.<sup>8</sup> This mixture was shaken overnight at room temperature (150 rpm). The two phases were then separated, and the aqueous phase was extracted one more time. The two obtained organic phases were pooled, and

the solvent was evaporated under vacuum. The crude extracts were dissolved (1.5 mg/mL) in LC–MS grade methanol for analysis.

### **LC–MS analysis and AHL quantification**

Chemical analyses were conducted with an Ultimate 3000™ UHPLC system (Thermo Fisher Scientific) coupled to an Orbitrap MS/MS FT Q-Exactive focus mass spectrometer. Analyses of extracts and standards (3 µL injected) were performed in the electrospray positive ionization mode in the 50–750  $m/z$  range in the centroid mode. The parameters were as follows: spray voltage: 3 kV; sheath flow rate: 75; auxiliary gas pressure: 20; capillary temperature: 350 °C; and heater temperature: 430 °C. The analysis was conducted in the FullMS data-dependent MS<sup>2</sup> mode (discovery mode). The resolution was set to 70,000 in the full MS mode, the AGC (automatic gain control) target was set to 10<sup>6</sup>, and the lock mass option was set for ions at  $m/z$  144.98215, corresponding to Cu(CH<sub>3</sub>CN)<sub>2</sub><sup>+</sup>. In MS<sup>2</sup>, the resolution was 17,500, the AGC target was set to 2×10<sup>5</sup>, the isolation window was 0.4  $m/z$ , and the normalized collision energy was stepped to 15, 30 and 40%, with 10 s dynamic exclusion. The UHPLC column was a Phenomenex Luna Omega Polar C18 1.6 µm, 150×2.1 mm. The column temperature was set to 42 °C, and the flow rate was 0.4 mL·min<sup>-1</sup>. The solvent system was a mixture of water (A) with increasing proportions of acetonitrile (B), and both solvents were modified with 0.1% formic acid. The gradient was as follows: 1% B 3 min before injection, then from 1 to 15 min, a linear increase of B up to 100% (curve 5), followed by 100% B for 5 min. Profiles were viewed using FreeStyle® 1.5 software (Thermo Fisher Scientific).

### **FBMN workflow and molecular networking analysis**

We used MZmine2 v2.51<sup>12–14</sup> to process the UHPLC–MS/MS data obtained from AHL standard analysis to obtain a feature detection and ion alignment table. MZmine2 data were then processed using the

Feature-Based Molecular Networking (FBMN) workflow in the GNPS (Global Natural Products Social Networking) platform.<sup>15,16</sup> The MZmine and FBMN parameters used for the generation of Figures 2 and 3 are detailed in the supporting information (Text files S1 and S2).

FBMN is a computational method that bridges mass spectrometry data processing tools for LC–MS/MS and molecular networking analysis on GNPS.<sup>17</sup> The FBMN workflow includes a high-throughput dereplication tool associated to comprehensive MS/MS libraries and finds analogs of known compounds in the library. The platform compares the MS/MS spectra of the unknown metabolites from samples with a library of MS/MS spectra generated from structurally characterized metabolites. Herein, this comparison is based upon the similarity cosine scoring of MS/MS spectra. The minimum cosine for linking two parent ions was set to 0.7. Our group implemented the GNPS platform with the MS<sup>2</sup> spectra of the 31 standard AHLs. Upon generating the MN, GNPS also annotated the AHLs automatically using the data we had provided to GNPS (Figure 2). The molecular network images (Figures 2 and 3) were generated with Cytoscape®,<sup>18</sup> an open source MN visualization software.

For the screening and annotation of natural AHLs (Figure 3), the MS1 alignment table (.csv file) obtained for the AHL standards was modified with arbitrary retention time and peak integration values (Table S1). The data obtained from the UHPLC–MS/MS analyses of the samples were then processed on MZmine2 using the same parameters described for the standards. The alignment table generated with MZmine2 was modified by inclusion, in Excel®, of Table S1. In the alignment table, 31 AHL rows with "row ID" from 1000001 to 1000031 (arbitrary values) were added, and a column "standards.raw peak area" was added to paste the arbitrary raw peak areas provided in Table S1 for standards, while the standard peak area was filled with zeros for the lines corresponding to sample ions. Meanwhile, the sample peak area was filled with zeros in standard lines 1000001 to 1000031. Figure S44 has been included in the supporting information for clarity.

Finally, the MS<sup>2</sup> file (.mgf) generated with MZmine2 was modified with a text editor by pasting the MS<sup>2</sup> spectra of the standards (Text file S3). Both files were processed by the FBMN workflow, as described for the standards. The result, visualized in Cytoscape, is shown in Figure 3. With these parameters, only short side chain AHLs (C2 and C4-HSL) were not clustered in the AHL MN.

## **RESULTS AND DISCUSSION**

### **Standard analysis**

First, we used a combination of 31 AHL standards (Table 1) to optimize the ionization parameters to increase the probability of detection of the homoserine moiety fragments shown in Figure 1.<sup>5,10</sup> The dominant ion observed for all AHL standards was the protonated molecular ion [M+H]<sup>+</sup>. The standard fragmentation data were registered in the spectral libraries of the GNPS platform to teach GNPS to dereplicate AHLs in its different workflows, and the spectra are also provided in the supporting information.

LC-MS/MS data obtained from the mixture of standards were processed with MZMine2 to obtain an MS/MS spectral summary file (in .mgf format) and a feature quantification table (.csv). These files were used with the GNPS FBMN workflow.

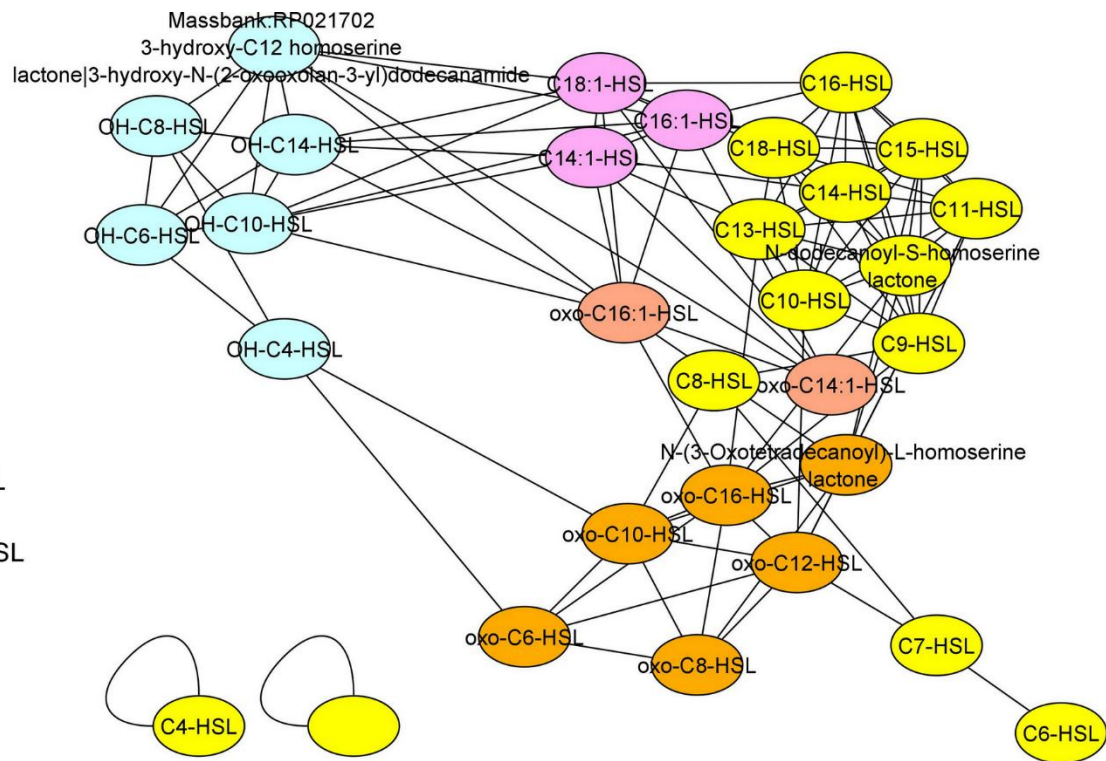


**Figure 2.** Molecular networking built by analysis of the AHL analytical standards. The annotations are from GNPS and included those recorded by us into the GNPS database. C2-HSL was not annotated. In the MN, AHLs were automatically grouped by type.

**Table 1.** Molecular formula, retention time ( $t_R$ ), theoretical and experimental  $m/z$  for the protonated molecular ion ( $[M+H]^+$ ), and limit of detection (LOD) for 31 *N*-acyl homoserine lactone (AHL) analytical standards

#	AHL	Molecular formula	$R_t$ (min)	Theoretical $[M+H]^+$	Exp. $[M+H]^+$	LOD (nM)
S1	C2-HSL	C <sub>6</sub> H <sub>9</sub> NO <sub>3</sub>	1.26	144.0655	144.0655	39
S2	C4-HSL	C <sub>8</sub> H <sub>13</sub> NO <sub>3</sub>	5.19	172.0968	172.0968	2477
S3	OH-C4-HLS	C <sub>8</sub> H <sub>13</sub> NO <sub>4</sub>	1.26	188.0917	188.0918	16
S4	C6-HSL	C <sub>10</sub> H <sub>17</sub> NO <sub>3</sub>	9.03	200.1283	200.1281	6
S5	OXO-C6-HSL	C <sub>10</sub> H <sub>15</sub> NO <sub>4</sub>	7.03	214.1074	214.1074	5
S6	C7-HSL	C <sub>11</sub> H <sub>19</sub> NO <sub>3</sub>	10.22	214.1438	214.1438	6
S7	OH-C6-HSL	C <sub>10</sub> H <sub>17</sub> NO <sub>4</sub>	6.77	216.1230	216.1231	54
S8	C8-HSL	C <sub>12</sub> H <sub>21</sub> NO <sub>3</sub>	11.24	228.1594	228.1595	6
S9	OXO-C8-HSL	C <sub>12</sub> H <sub>19</sub> NO <sub>4</sub>	9.74	242.1387	242.1387	11
S10	C9-HSL	C <sub>13</sub> H <sub>23</sub> NO <sub>3</sub>	12.13	242.1751	242.1751	5
S11	OH-C8-HSL	C <sub>12</sub> H <sub>21</sub> NO <sub>4</sub>	9.25	244.1543	244.1544	5
S12	C10-HSL	C <sub>14</sub> H <sub>25</sub> NO <sub>3</sub>	12.93	256.1907	256.1908	21
S13	OXO-C10-HSL	C <sub>14</sub> H <sub>23</sub> NO <sub>4</sub>	11.68	270.1694	270.1702	7
S14	C11-HSL	C <sub>15</sub> H <sub>27</sub> NO <sub>3</sub>	13.67	270.2064	270.2065	6
S15	OH-C10-HSL	C <sub>14</sub> H <sub>25</sub> NO <sub>4</sub>	11.14	272.1856	272.1858	5
S16	C12-HSL	C <sub>16</sub> H <sub>29</sub> NO <sub>3</sub>	14.37	284.2220	284.2222	4
S17	OXO-C12-HSL	C <sub>16</sub> H <sub>27</sub> NO <sub>4</sub>	13.24	298.2013	298.2015	4
S18	C13-HSL	C <sub>17</sub> H <sub>31</sub> NO <sub>3</sub>	15.03	298.2377	298.2379	4
S19	OH-C12-HSL	C <sub>16</sub> H <sub>29</sub> NO <sub>4</sub>	12.71	300.2169	300.2171	4
S20	C14:1-HSL	C <sub>18</sub> H <sub>31</sub> NO <sub>3</sub>	14.83	310.2377	310.2379	3
S21	C14-HSL	C <sub>18</sub> H <sub>33</sub> NO <sub>3</sub>	15.67	312.2533	312.2535	4
S22	OXO-C14:1-HSL	C <sub>18</sub> H <sub>29</sub> NO <sub>4</sub>	13.92	324.2169	324.2171	4
S23	OXO-C14-HSL	C <sub>18</sub> H <sub>31</sub> NO <sub>4</sub>	14.59	326.2326	326.2328	3
S24	C15-HSL	C <sub>19</sub> H <sub>35</sub> NO <sub>3</sub>	16.27	326.2690	326.2692	5
S25	OH-C14-HSL	C <sub>18</sub> H <sub>33</sub> NO <sub>4</sub>	14.11	328.2482	328.2484	2
S26	C16:1-HSL	C <sub>20</sub> H <sub>35</sub> NO <sub>3</sub>	16.01	338.2690	338.2691	3
S27	C16-HSL	C <sub>20</sub> H <sub>37</sub> NO <sub>3</sub>	16.83	340.2846	340.2848	4
S28	OXO-C16:1-HSL	C <sub>20</sub> H <sub>33</sub> NO <sub>4</sub>	15.00	352.2482	352.2484	6
S29	OXO-C16-HSL	C <sub>20</sub> H <sub>35</sub> NO <sub>4</sub>	15.83	354.2639	354.2641	5
S30	C18:1-HSL	C <sub>22</sub> H <sub>39</sub> NO <sub>3</sub>	17.08	366.3003	366.3004	4
S31	C18-HSL	C <sub>22</sub> H <sub>41</sub> NO <sub>3</sub>	17.81	368.3159	368.3161	4

The network obtained (Figure 2) confirmed that the method allowed the tool to recognize the fragmentation patterns of parent ions corresponding to standard AHLs and to reconstitute a network according to the degree of similarity between fragmentation spectra. In the GNPS Molecular Networking tools, the annotation of the ions is given by MS-Cluster, an algorithm used by GNPS to collapse nearly identical MS spectra with the same precursor ion  $m/z$  into a single "consensus" or "clustered" spectrum regardless of their chromatographic retention time. The FBMN workflow, however, allows the detection of isomers that are separated chromatographically, even if they will be annotated identically by GNPS.

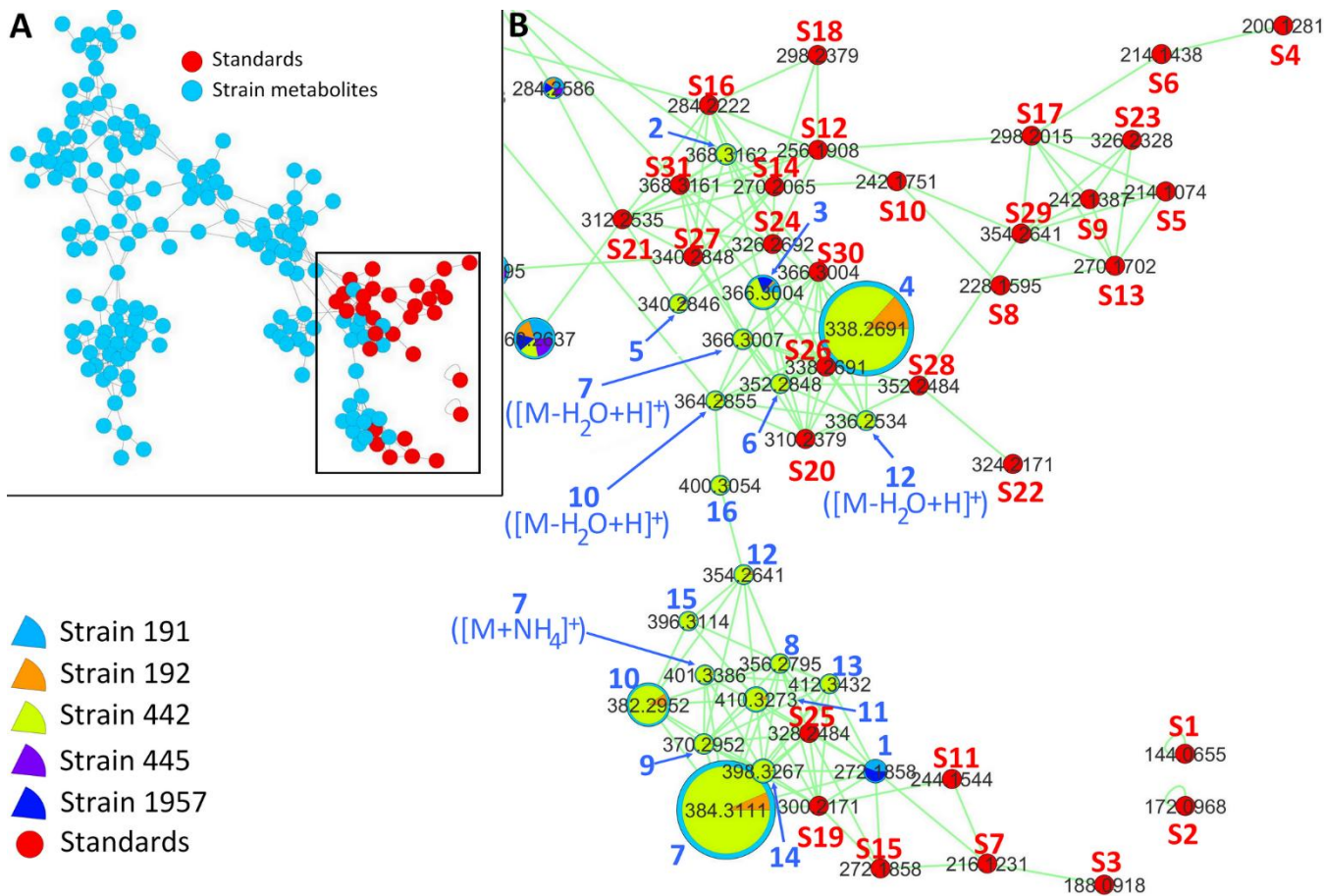
The network shows that 30 AHLs were annotated correctly by GNPS and grouped in one single network (Figure 2). Subtle structural differences also revealed subnetworks within the AHL network, in which 3-oxo- or 3-hydroxy-AHLs were grouped. C6- and C7-HSL bound to the network but did not regroup with the other *N*-acyl-HSLs (yellow clusters). However, they were correctly annotated by the dereplication tool. C4-HSL was also correctly annotated but was not bound to the network of AHLs, while C2-AHL was separated and was not annotated automatically. Overall, the automatic MN analysis and dereplication tool should be able to annotate any AHL with an acyl side chain of at least 4 carbons but will fail to annotate C2-HSL.

### **Detection and annotation of AHLs in bacterial extracts**

Our next goal was to propose an untargeted metabolomics method to search and annotate known and unknown AHLs from bacterial extracts. Five strains were cultivated in triplicate, eventually yielding 15 extracts that were analyzed following the same protocol as for the standards. The MN was constructed with the FBMN tool, including the standard MS<sup>2</sup> spectra provided in the text file in the supporting information (Figure 3). The compilation of the standards and sample tables allowed us to create a network similar to the one in Figure 2 in which the strain AHL ion network was nested within the standard net-

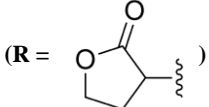
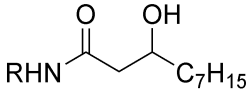
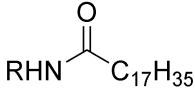
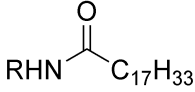
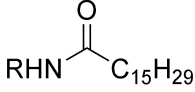
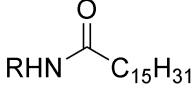
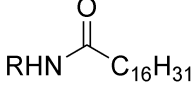
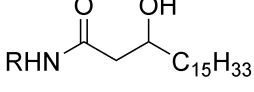
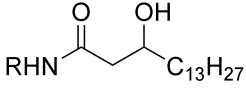
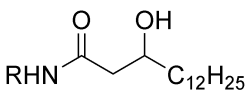
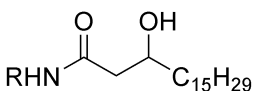
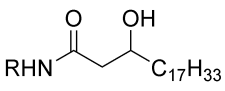
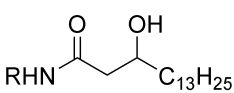
work. This tool thus allowed the annotation of AHLs for which standards were not commercially available and would allow laboratories that do not have the standards to annotate AHLs.

Figure 3B is an enlargement of the AHL-including part of the larger network shown in Figure 3A. The AHLs were assigned to each strain with pie charts in the nodes, and the size of each node was assigned to the peak integration value in the extracted ion chromatogram (EIC). When the same AHL was present in the list of standards and in a strain extract, it appeared as two different points very close to each other. This is the case for compounds **1-5**. Compounds **6-16** did not correspond to standards but were grouped with AHLs in the MN and were annotated as AHLs after manual verification of their molecular formula and MS<sup>2</sup> spectra to confirm the presence of the 4 diagnostic fragments at  $m/z$  102.055, 84.045, 74.061, and 56.050.<sup>8,10</sup>



**Figure 3.** MN generated from bacterial extract profiling and the standard AHL MS<sup>2</sup> data text file provided in the supporting information. Unless otherwise mentioned, the ion mass reported on the figure corresponds to the protonated molecular ion of the corresponding AHL.

**Table 2. Experimental  $m/z$ , molecular formula, proposed structure and side chain for the 16 natural AHLs found in the MN (Figure 3).**

#	MN $m/z$	Ion type	$t_R$ (min)	Molecular formula	Proposed structure		Annotation	Std. <sup>a</sup>	Strains
					(R =  )				
1	272.1856	[M+H] <sup>+</sup>	11.14	C <sub>14</sub> H <sub>25</sub> NO <sub>4</sub>			OH-C10-HSL	S15	191, 445, 1957
2	368.3159	[M+H] <sup>+</sup>	17.81	C <sub>22</sub> H <sub>41</sub> NO <sub>3</sub>			C18-HSL	S31	191, 192, 442, 1957
3	366.3003	[M+H] <sup>+</sup>	17.08	C <sub>22</sub> H <sub>39</sub> NO <sub>3</sub>			C18:1-HSL	S30	191, 192, 442, 1957
4	338.269	[M+H] <sup>+</sup>	16.01	C <sub>20</sub> H <sub>35</sub> NO <sub>3</sub>			C16:1-HSL	S26	191, 192, 442, 445
5	340.2846	[M+H] <sup>+</sup>	16.83	C <sub>20</sub> H <sub>37</sub> NO <sub>3</sub>			C16-HSL	S27	192, 442, 1957
6	352.2848	[M+H] <sup>+</sup>	16.71	C <sub>21</sub> H <sub>37</sub> NO <sub>3</sub>			C17:1-HSL		192, 442
7	384.3111	[M+H] <sup>+</sup>	16.76	C <sub>22</sub> H <sub>41</sub> NO <sub>4</sub>			OH-C18-HSL		192, 442, 445
7	401.3386	[M+NH <sub>4</sub> ] <sup>+</sup>	16.76	C <sub>22</sub> H <sub>45</sub> N <sub>2</sub> O <sub>4</sub>					192,442
7	366.3007	[M-H <sub>2</sub> O+H] <sup>+</sup>	16.76	C <sub>22</sub> H <sub>39</sub> NO <sub>3</sub>					192,442
8	356.2797	[M+H] <sup>+</sup>	15.56	C <sub>20</sub> H <sub>37</sub> NO <sub>4</sub>			OH-C16-HSL		192, 442
9	370.2952	[M+H] <sup>+</sup>	16.19	C <sub>21</sub> H <sub>39</sub> NO <sub>4</sub>			OH-C15-HSL		192, 442
10	382.2942	[M+H] <sup>+</sup>	15.92	C <sub>22</sub> H <sub>39</sub> NO <sub>4</sub>			OH-C18:1-HSL		192, 442, 1957
10	364.2855	[M-H <sub>2</sub> O+H] <sup>+</sup>	15.92	C <sub>22</sub> H <sub>37</sub> NO <sub>3</sub>					192, 442, 1957
11	410.3273	[M+H] <sup>+</sup>	16.95	C <sub>24</sub> H <sub>43</sub> NO <sub>4</sub>			OH-C20:1-HSL		192, 442
12	354.264	[M+H] <sup>+</sup>	14.33	C <sub>20</sub> H <sub>35</sub> NO <sub>4</sub>			OH-C16:1-HSL		442
12	336.2534	[M-H <sub>2</sub> O+H] <sup>+</sup>	14.33	C <sub>20</sub> H <sub>33</sub> NO <sub>3</sub>					

13	412.3432	[M+H] <sup>+</sup>	17.81	C <sub>24</sub> H <sub>45</sub> NO <sub>4</sub>		OH-C20-HSL	442
14	398.3265	[M+H] <sup>+</sup>	17.32	C <sub>23</sub> H <sub>43</sub> NO <sub>4</sub>		OH-C19-HSL	442
15	396.311	[M+H] <sup>+</sup>	16.45	C <sub>23</sub> H <sub>41</sub> NO <sub>4</sub>		OH-C19:1-HSL	442
16	400.3074	[M+H] <sup>+</sup>	14.30	C <sub>22</sub> H <sub>41</sub> NO <sub>5</sub>		2-OH-C18-HSL	442

<sup>a</sup>Std.: The corresponding AHL was present in the list of standards (Table 1), allowing for level 1 annotation.<sup>19</sup> Other annotations (compounds **6-16**) are level 2.

Additionally, since the oxo-AHLs were separated from the hydroxyl groups in the MN, the method was effective in differentiating possible oxo and OH isomers. For example, compound **10** was annotated as OH-C18:1-HSL and not as oxo-C18-HSL based on its neighbors in the MN. It is interesting to note that the network also grouped 1 ammonium adduct of compound **7** and 3 dehydro forms for compounds **7**, **10**, and **16**. The in-source dehydration products, in particular, may be mistaken for native AHLs. Identical retention time and peak shapes in the extracted ion chromatograms confirmed the annotation of these ions as in-source fragments. Furthermore, Figure 3 graphically shows that compound **4** corresponding to C16:1-HSL (**S26**) and an unknown AHL at *m/z* 384.3111(**7**) were the major metabolites in these strains. Based on the molecular formula and fragmentation pattern, **7** was annotated as an OH-C18-HSL. Overall, the propagation of the annotation from the standards to the unknowns quickly allowed for annotation of all of the natural AHLs from the 4 strains (Table 2). Figure 3 also shows that the extract with the greatest diversity of AHLs was that of strain BBCC442. Eventually, the AHLs could be quantified according to external calibration curves obtained with the standards (results in Table S2). We were able to establish that the extracted ion chromatogram peak area for each [M+H]<sup>+</sup> ion was proportional to the concentration of the corresponding AHL in the mixture. It was therefore possible to simply assess which are the major AHLs – presumably carrying the quorum sensing activity – in each strain.

## CONCLUSIONS

This method was found to be a powerful and straightforward approach for the detection and annotation of known and unknown AHLs in a bacterial sample. It is largely based on the automatic annotation tool provided by the GNPS platform. In the case of new/unknown AHLs, annotation was performed by propagation along a MN built from strain metabolomic profiles and standard analytical data provided in the supporting information. The FBMN figure provided a direct view of the diversity and the relative abundances of the different known and unknown AHLs in the bacterial cultures.

We anticipate that the method developed for this study could be of great assistance in the automatic annotation and relative quantification of known and unknown AHLs from bacterial cultures. If needed, we are also making the raw analysis file of the mixture of standards used for the development of this method available to the community upon request to the corresponding author.

## ASSOCIATED CONTENT

### Supporting Information

The Supporting Information is available free of charge on the ACS Publications website.

FIGURE S1- MS/MS spectrum of C2-HSL protonated molecular ion  $[(S1+H)^+]$ ; FIGURE S2 - MS/MS spectrum of C4-HSL protonated molecular ion  $[(S2+H)^+]$ ; FIGURE S3 - MS/MS spectrum of OH-C4-HSL protonated molecular ion  $[(S3+H)^+]$ ; FIGURE S4 - MS/MS spectrum of C6-HSL protonated molecular ion  $[(S4+H)^+]$ ; FIGURE S5 - MS/MS spectrum of oxo-C6-HSL protonated molecular ion  $[(S5+H)^+]$ ; FIGURE S6 – MS/MS spectrum of C7-HSL protonated molecular ion  $[(S6+H)^+]$ ; FIGURE S7 - MS/MS spectrum of OH-C6-HSL protonated molecular ion  $[(S7+H)^+]$ ; FIGURE S8 – MS/MS spectrum of C8-HSL protonated molecular ion  $[(S8+H)^+]$ ; FIGURE S9 – MS/MS spectrum of oxo-C8-HSL protonated molecular ion  $[(S9+H)^+]$ ; FIGURE S10 – MS/MS spectrum of C9-HSL protonated mo-

lecular ion [(S10+H)<sup>+</sup>]; FIGURE S11 – MS/MS spectrum of OH-C8-HSL protonated molecular ion [(S11+H)<sup>+</sup>]; FIGURE S12 – MS/MS spectrum of C10-HSL protonated molecular ion [(S12+H)<sup>+</sup>]; FIGURE S13 – MS/MS spectrum of oxo-C10-HSL protonated molecular ion [(S13+H)<sup>+</sup>]; FIGURE S14 – MS/MS spectrum of C11-HSL protonated molecular ion [(S14+H)<sup>+</sup>]; FIGURE S15 – MS/MS spectrum of OH-C10-HSL protonated molecular ion [(S15+H)<sup>+</sup>]; FIGURE S16 – MS/MS spectrum of C12-HSL protonated molecular ion [(S16+H)<sup>+</sup>]; FIGURE S17 - MS/MS spectrum of oxo-C12-HSL protonated molecular ion [(S17+H)<sup>+</sup>]; FIGURE S18 - MS/MS spectrum of C13-HSL protonated molecular ion [(S18+H)<sup>+</sup>]; FIGURE S19 - MS/MS spectrum of OH-C12-HSL protonated molecular ion [(S19+H)<sup>+</sup>]; FIGURE S20 - MS/MS spectrum of C14:1-HSL protonated molecular ion [(S20+H)<sup>+</sup>]; FIGURE S21 - MS/MS spectrum of C14-HSL protonated molecular ion [(S21+H)<sup>+</sup>]; FIGURE S22 - MS/MS spectrum of oxo-C14:1-HSL protonated molecular ion [(S22+H)<sup>+</sup>]; FIGURE S23 - MS/MS spectrum of oxo-C14-HSL protonated molecular ion [(S23+H)<sup>+</sup>]; FIGURE S24 - MS/MS spectrum of C15-HSL protonated molecular ion [(S24+H)<sup>+</sup>]; FIGURE S25 - MS/MS spectrum of OH-C14-HSL protonated molecular ion [(S25+H)<sup>+</sup>]; FIGURE S26 - MS/MS spectrum of C16:1-HSL protonated molecular ion [(S26+H)<sup>+</sup>]; FIGURE S27 - MS/MS spectrum of C16-HSL protonated molecular ion [(S27+H)<sup>+</sup>]; FIGURE S28 - MS/MS spectrum of oxo-C16:1-HSL protonated molecular ion [(S28+H)<sup>+</sup>]; FIGURE S29 - MS/MS spectrum of oxo-C16-HSL protonated molecular ion [(S29+H)<sup>+</sup>]; FIGURE S30 - MS/MS spectrum of C18:1-HSL protonated molecular ion [(S30+H)<sup>+</sup>]; FIGURE S31 – MS/MS spectrum of C18-HSL protonated molecular ion [(S31+H)<sup>+</sup>]; FIGURE S32 - MS/MS spectrum of ion at *m/z* 352.2848 [(6+H)<sup>+</sup>]; FIGURE S33 - MS/MS spectrum of ion at *m/z* 384.3009 [(7+H)<sup>+</sup>]; FIGURE S34 - MS/MS spectrum of ion at *m/z* 401.3374 [(7+NH4)<sup>+</sup>]; FIGURE S35 - MS/MS spectrum of ion at *m/z* 356.2797 [(8+H)<sup>+</sup>]; FIGURE S36 - MS/MS spectrum of ion at *m/z* 370.2950 [(9+H)<sup>+</sup>]; FIGURE S37 - MS/MS spectrum of ion at *m/z* 382.2952 [(10+H)<sup>+</sup>]; FIGURE S38 - MS/MS spectrum of ion at *m/z* 410.3266 [(11+H)<sup>+</sup>]; FIGURE S39 - MS/MS spectrum of ion at *m/z* 354.2641 [(12+H)<sup>+</sup>]; FIGURE

S40 - MS/MS spectrum of ion at  $m/z$  412.3423 [(13+H)<sup>+</sup>]; FIGURE S41 - MS/MS spectrum of ion at  $m/z$  398.3265 [(14+H)<sup>+</sup>]; FIGURE S42 - MS/MS spectrum of ion at  $m/z$  396.3110 [(15+H)<sup>+</sup>]; FIGURE S43 - MS/MS spectrum of ion at  $m/z$  400.3074 [(16+H)<sup>+</sup>]; TEXT FILE S1 – Important parameters for MZmine2 data processing; TEXT FILE S2 – Important parameters for FBMN analysis; TABLE S1 – Table of the 31 standard AHLs for inclusion into the .csv file generated by MZmine2; FIGURE S44 – Illustration of .csv file modification for inclusion of standard AHLs; TEXT FILE S3 - AHLs MS2 spectral data for inclusion into the .mgf file generated by MzMine2 after processing. This dataset should be pasted at the end of the file built from the samples; TABLE S2. Measured concentrations (mM) of known AHLs in bacterial extracts (DOCX).

## **AUTHOR INFORMATION**

### **Corresponding Author**

\* Alice M. S. Rodrigues – Sorbonne Université/CNRS, LBBM, Observatoire Océanologique, 66650 Banyuls-sur-Mer, France; [orcid.org/0000-0001-7671-1261](https://orcid.org/0000-0001-7671-1261); Email: [rodrigues@obs-banyuls.fr](mailto:rodrigues@obs-banyuls.fr).

### **Author Contributions**

A.M.S.R., L.I., C.M., M.D., P.P., D.S.: investigation, review, and editing; R.L., K.E.: review and editing; A.M.S.R., D.S.: formal analysis, writing review, and editing; and A.M.S.R.: conceptualization, investigation, and writing the original draft. The manuscript was written through contributions of all authors. All authors have given approval to the final version of the manuscript.

## **ACKNOWLEDGMENT**

This work has benefited from a joint Agence Nationale de la Recherche - Swiss National Science Foundation (ANR-SNF) grant (SECIL, ref ANR-15-CE21-0016 and SNF N° 310030E-164289).

## **REFERENCES**

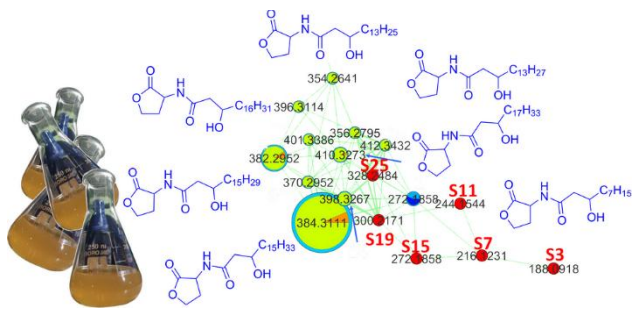
- (1) Miller, M. B.; Bassler, B. L. Quorum Sensing in Bacteria. *Ann. Rev. Microbiol.* **2001**, *55* (1), 165–199.
- (2) Lami, R. Chapter 3 - Quorum Sensing in Marine Biofilms and Environments. In *Quorum Sensing*; Tommonaro, G., Ed.; Academic Press, 2019; pp 55–96.
- (3) Aframian, N.; Eldar, A. A Bacterial Tower of Babel: Quorum-Sensing Signaling Diversity and Its Evolution. *Ann. Rev. Microbiol.* **2020**, *74* (1), 587–606.
- (4) Venturi, V.; Ahmer, B. M. M. Editorial: LuxR Solos Are Becoming Major Players in Cell–Cell Communication in Bacteria. *Front. Cell. Infect. Microbiol.* **2015**, *5*, 89.
- (5) Cataldi, T. R. I.; Bianco, G.; Abate, S.; Losito, I. Identification of Unsaturated N-Acylhomoserine Lactones in Bacterial Isolates of *Rhodobacter Sphaeroides* by Liquid Chromatography Coupled to Electrospray Ionization-Hybrid Linear Ion Trap-Fourier Transform Ion Cyclotron Resonance Mass Spectrometry. *Rapid Commun. Mass Spectrom.* **2011**, *25* (13), 1817–1826.
- (6) Steindler, L.; Venturi, V. Detection of Quorum-Sensing N-Acyl Homoserine Lactone Signal Molecules by Bacterial Biosensors. *FEMS Microbiol. Lett.* **2007**, *266* (1), 1–9.
- (7) Wang, J.; Ding, L.; Li, K.; Schmieder, W.; Geng, J.; Xu, K.; Zhang, Y.; Ren, H. Development of an Extraction Method and LC–MS Analysis for N-Acylated-L-Homoserine Lactones (AHLs) in Wastewater Treatment Biofilms. *J. Chromatogr. B* **2017**, *1041–1042*, 37–44.
- (8) Doberva, M.; Stien, D.; Sorres, J.; Hue, N.; Sanchez-Ferandin, S.; Eparvier, V.; Ferandin, Y.; Lebaron, P.; Lami, R. Large Diversity and Original Structures of Acyl-Homoserine Lactones in Strain MOLA 401, a Marine *Rhodobacteraceae* Bacterium. *Front. Microbiol.* **2017**, *8*, 1152. <https://doi.org/10.3389/fmicb.2017.01152>.
- (9) Lépine, F.; Milot, S.; Groleau, M.-C.; Déziel, E. Liquid Chromatography/Mass Spectrometry (LC/MS) for the Detection and Quantification of N-Acyl-L-Homoserine Lactones (AHLs) and 4-

- Hydroxy-2-Alkylquinolines (HAQs). In *Quorum Sensing: Methods and Protocols*; Leoni, L., Rampioni, G., Eds.; Springer New York: New York, NY, 2018; pp 49–59.
- (10) Patel, N. M.; Moore, J. D.; Blackwell, H. E.; Amador-Noguez, D. Identification of Unanticipated and Novel *N*-Acyl L-Homoserine Lactones (AHLs) Using a Sensitive Non-Targeted LC-MS/MS Method. *PLoS One* **2016**, *11* (10), e0163469.
- (11) Microorganismes unicellulaires | EMBRC France <https://www.embrc-france.fr/fr/our-services/supply-biological-resources/microorganisms/microorganismes-unicellulaires> (accessed 2021 -10 -25).
- (12) Pluskal, T.; Castillo, S.; Villar-Briones, A.; Orešič, M. MZmine 2: Modular Framework for Processing, Visualizing, and Analyzing Mass Spectrometry-Based Molecular Profile Data. *BMC Bioinf.* **2010**, *11* (1), 395.
- (13) Katajamaa, M.; Miettinen, J.; Orešič, M. MZmine: Toolbox for Processing and Visualization of Mass Spectrometry Based Molecular Profile Data. *Bioinformatics* **2006**, *22* (5), 634–636.
- (14) MZmine 2 <http://mzmine.github.io/> (accessed 2021 -10 -25).
- (15) Wang, M.; Carver, J. J.; Phelan, V. V.; Sanchez, L. M.; Garg, N.; Peng, Y.; Nguyen, D. D.; Watrous, J.; Kaponov, C. A.; Luzzatto-Knaan, T.; Porto, C.; Bouslimani, A.; Melnik, A. V.; Meehan, M. J.; Liu, W.-T.; Crüsemann, M.; Boudreau, P. D.; Esquenazi, E.; Sandoval-Calderón, M.; Kersten, R. D.; Pace, L. A.; Quinn, R. A.; Duncan, K. R.; Hsu, C.-C.; Floros, D. J.; Gavilan, R. G.; Kleingrewe, K.; Northen, T.; Dutton, R. J.; Parrot, D.; Carlson, E. E.; Aigle, B.; Michelsen, C. F.; Jelsbak, L.; Sohlenkamp, C.; Pevzner, P.; Edlund, A.; McLean, J.; Piel, J.; Murphy, B. T.; Gerwick, L.; Liaw, C.-C.; Yang, Y.-L.; Humpf, H.-U.; Maansson, M.; Keyzers, R. A.; Sims, A. C.; Johnson, A. R.; Sidebottom, A. M.; Sedio, B. E.; Klitgaard, A.; Larson, C. B.; Boya P, C. A.; Torres-Mendoza, D.; Gonzalez, D. J.; Silva, D. B.; Marques, L. M.; Demarque, D. P.; Pociute, E.; O'Neill, E. C.; Briand, E.; Helfrich, E. J. N.; Granatosky, E. A.; Glukhov, E.; Ryffel, F.; Houson,

H.; Mohimani, H.; Kharbush, J. J.; Zeng, Y.; Vorholt, J. A.; Kurita, K. L.; Charusanti, P.; McPhail, K. L.; Nielsen, K. F.; Vuong, L.; Elfeki, M.; Traxler, M. F.; Engene, N.; Koyama, N.; Vining, O. B.; Baric, R.; Silva, R. R.; Mascuch, S. J.; Tomasi, S.; Jenkins, S.; Macherla, V.; Hoffman, T.; Agarwal, V.; Williams, P. G.; Dai, J.; Neupane, R.; Gurr, J.; Rodríguez, A. M. C.; Lamsa, A.; Zhang, C.; Dorrestein, K.; Duggan, B. M.; Almaliti, J.; Allard, P.-M.; Phapale, P.; Nothias, L.-F.; Alexandrov, T.; Litaudon, M.; Wolfender, J.-L.; Kyle, J. E.; Metz, T. O.; Peryea, T.; Nguyen, D.-T.; VanLeer, D.; Shinn, P.; Jadhav, A.; Müller, R.; Waters, K. M.; Shi, W.; Liu, X.; Zhang, L.; Knight, R.; Jensen, P. R.; Palsson, B. Ø.; Pogliano, K.; Linington, R. G.; Gutiérrez, M.; Lopes, N. P.; Gerwick, W. H.; Moore, B. S.; Dorrestein, P. C.; Bandeira, N. Sharing and Community Curation of Mass Spectrometry Data with Global Natural Products Social Molecular Networking. *Nat. Biotechnol.* **2016**, *34* (8), 828–837.

- (16) GNPS - Analyze, Connect, and Network with your Mass Spectrometry Data <https://gnps.ucsd.edu/> (accessed 2021 -10 -25).
- (17) Nothias, L.-F.; Petras, D.; Schmid, R.; Dührkop, K.; Rainer, J.; Sarvepalli, A.; Protsyuk, I.; Ernst, M.; Tsugawa, H.; Fleischauer, M.; Aicheler, F.; Aksenov, A. A.; Alka, O.; Allard, P.-M.; Barsch, A.; Cachet, X.; Caraballo-Rodriguez, A. M.; Da Silva, R. R.; Dang, T.; Garg, N.; Gauglitz, J. M.; Gurevich, A.; Isaac, G.; Jarmusch, A. K.; Kameník, Z.; Kang, K. B.; Kessler, N.; Koester, I.; Korf, A.; Le Gouellec, A.; Ludwig, M.; Martin H., C.; McCall, L.-I.; McSayles, J.; Meyer, S. W.; Mohimani, H.; Morsy, M.; Moyne, O.; Neumann, S.; Neuweiger, H.; Nguyen, N. H.; Nothias-Esposito, M.; Paolini, J.; Phelan, V. V.; Pluskal, T.; Quinn, R. A.; Rogers, S.; Shrestha, B.; Tripathi, A.; van der Hooft, J. J. J.; Vargas, F.; Weldon, K. C.; Witting, M.; Yang, H.; Zhang, Z.; Zubeil, F.; Kohlbacher, O.; Böcker, S.; Alexandrov, T.; Bandeira, N.; Wang, M.; Dorrestein, P. C. Feature-Based Molecular Networking in the GNPS Analysis Environment. *Nat. Methods* **2020**, *17* (9), 905–908.

- (18) Otasek, D.; Morris, J. H.; Bouças, J.; Pico, A. R.; Demchak, B. Cytoscape Automation: Empowering Workflow-Based Network Analysis. *Genome Biol.* **2019**, *20* (1), 185.
- (19) Sumner, L. W.; Amberg, A.; Barrett, D.; Beale, M. H.; Beger, R.; Daykin, C. A.; Fan, T. W.-M.; Fiehn, O.; Goodacre, R.; Griffin, J. L.; Hankemeier, T.; Hardy, N.; Harnly, J.; Higashi, R.; Kopka, J.; Lane, A. N.; Lindon, J. C.; Marriott, P.; Nicholls, A. W.; Reily, M. D.; Thaden, J. J.; Viant, M. R. Proposed Minimum Reporting Standards for Chemical Analysis Chemical Analysis Working Group (CAWG) Metabolomics Standards Initiative (MSI). *Metabolomics* **2007**, *3* (3), 211–221.



## For Table of Contents Only

I confirm that the TOC graphic is original and was created 100 % by the authors.